Published in final edited form as:
J Am Chem Soc. 2009 April 8; 131(13): 4783–4787. doi:10.1021/ja809086q.

PEG Branched Polymer for Functionalization of Nanomaterials with Ultralong Blood Circulation

Giuseppe Prencipe, **Scott M. Tabakman**, **Kevin Welsher**, **Zhuang Liu**, **Andrew P. Goodwin**, **Li Zhang**, **Joy Henry**, and **Hongjie Dai***
Department of Chemistry, Stanford University, Keck Science Building, Rm 125, 380 Roth Way, Stanford, California 94305

Abstract

Nanomaterials have been actively pursued for biological and medical applications in recent years. Here, we report the synthesis of several new poly(ethylene glycol) grafted branched polymers for functionalization of various nanomaterials including carbon nanotubes, gold nanoparticles (NPs), and gold nanorods (NRs), affording high aqueous solubility and stability for these materials. We synthesize different surfactant polymers based upon poly(γ-glutamic acid) (γPGA) and poly(maleic anhydride-*alt*-1-octadecene) ($PMHC_{18}$). We use the abundant free carboxylic acid groups of γPGA for attaching lipophilic species such as pyrene or phospholipid, which bind to nanomaterials via robust physisorption. Additionally, the remaining carboxylic acids on γPGA or the amine-reactive anhydrides of $PMHC_{18}$ are then PEGylated, providing extended hydrophilic groups, affording polymeric amphiphiles. We show that single-walled carbon nanotubes (SWNTs), Au NPs, and NRs functionalized by the polymers exhibit high stability in aqueous solutions at different pH values, at elevated temperatures, and in serum. Morever, the polymer-coated SWNTs exhibit remarkably long blood circulation ($t_{1/2}$ = 22.1 h) upon intravenous injection into mice, far exceeding the previous record of 5.4 h. The ultralong blood circulation time suggests greatly delayed clearance of nanomaterials by the reticuloendothelial system (RES) of mice, a highly desired property for in vivo applications of nanomaterials, including imaging and drug delivery.

Introduction

Nanostructures including SWNTs, Au NPs, and Au NRs are currently being explored for biomedical applications, including in vivo delivery (e.g., drugs,[1,2] proteins, peptides,[3–5] and nucleic acids[2,4–9]), biological detection of proteins,[10–12] and in vivo imaging.[13] Most inorganic nanomaterials are not soluble in physiological buffers and require functionalization by thiols or surfactants to obtain biocompatibility. Many surfactant coatings become unstable in serum or upon removing the excess of the coating molecule. PEGylation is a common strategy to impart functionality, water solubility, and biocompatibility.[14–17] Even so, in vivo, most of the existing functionalization methods of nanomaterials suffer from rapid uptake by the reticuloendothelial system (RES) and short blood circulation times. Sufficient blood circulation time is critical to both imaging and in vivo delivery.

In recent years, advances have been made toward the use of polymeric amphiphiles to coat nanomaterials noncovalently. For SWNTs, noncovalent functionalization is necessary to

hdai1@stanford.edu.

Supporting Information Available: Materials and methods, as well as CMCs and dynamic light scattering spectra, AFM images and the PLE spectra of suspensions of SWNTs via **2** and **3**, and the quenching of pyrene fluorescence on SWNTs and gold NPs. This material is available free of charge via the Internet at http://pubs.acs.org.

preserve the intrinsic physical properties of SWNTs, including near-infrared fluorescence and Raman scattering, useful for biomedical imaging.[18] To this end, SWNTs have been incorporated into micelles formed by various surfactants in aqueous solutions, such as lipids,[19,20] sugars,[21] proteins,[22,23] DNA,[24,25] and polymers such as poly(ethylene glycol) (PEG).[26,27] Also, it has been found that densely coating nanomaterial surfaces with PEG[28,29] increases in vivo circulation times, likely by resisting clearance via the RES. Still, much room exists to optimize noncovalent nanomaterial surface coating, improving the circulation behavior of SWNTs for in vivo biomedical applications including tumor targeting, imaging, and therapy.

Similarly to SWNTs, inorganic colloidal nanoparticles, such as gold nanoparticles (NPs) or gold nanorods, have been extensively investigated for two decades and have found application largely in detection schemes for DNA,[7–9] proteins,[10,11] and other biomolecular analytes. NPs and NRs have also been used in single-particle coding and tracking experiments in vitro[30–35] and in vivo.[36] These applications require robust, aqueous nanoparticle suspensions, which have relied upon surface passivation by small molecules,[37–42] lipids,[43–45] surface silanization,[46–49] and amphiphilic polymer coatings. There is significant ongoing research regarding the synthesis of stabilized Au NPs in the presence or in the absence of thiol ligands.[50–52] Pyrene-containing and phospholipid-coating moieties have been used extensively for binding to carbon nanotubes[13,28,53,54] and gold nanoparticles,[55] due to strong interactions including van der Waals forces, π–π stacking, charge transfer, and/or hydrophobic interactions.[28,56,57]

Here, we report the synthesis of several new poly(ethylene glycol) grafted branched polymers (Figure 1) based upon poly(γ-glutamic acid) (γPGA) and poly(maleic anhydride-*alt*-1-octadecene) ($PMHC_{18}$). Poly-γ-glutamic acid is a naturally occurring biomaterial, produced by microbial fermentation.[58] γPGA is water soluble, biodegradable, nontoxic, and edible. We propose that a portion of the free carboxylic acids of γPGA could first be coupled to lipophilic groups for binding to nanomaterials via hydrophobic and van der Waals interactions, while the remaining carboxylic acids can be conjugated to PEG, providing enhanced aqueous solubility and further biocompatibility.[59] In the case of **1**, the copolymer itself contains an alternating hydrophobic unit, the C_{18} chain. Specifically, maleic anhydride groups may be reacted with primary amine-terminated PEG, and remaining carboxylic acids can be conjugated to PEG via amidation chemistry.

We found that not only was this material able to form self-assemblies easily in water, but it also formed stable coatings on carbon nanotubes, gold nanoparticles, and gold nanorods. These polymer–nanomaterial coatings showed stability to a range of pH values, salt conditions, and introduction of serum. Finally, polymer-coated SWNTs exhibit remarkably long blood circulation ($t_{1/2}$ = 22.1 h) upon intravenous injection into mice when compared with the previous record of 5.4 h.

Results and Discussion

Synthesis of Polymers

Pyrene and phospholipid were chosen as lipophilic groups for attachment to biocompatible polymers. In the first synthetic step (see Supporting Information for methods), we used the free carboxylic acid of γPGA (M_n ~ 430 kDa) to couple 1-methylaminopyrene via EDC amidation. In a second step, we used the remaining carboxylic acid groups of γPGA to attach amine-terminated poly(ethylene glycol) methyl ethers (mPEG-NH_2, M_w = 5000) to afford the compound **2**. The average number of pyrene moieties grafted to γPGA chains was determined by ^{1}H NMR and estimated to be ~30%, with ~70% of the γPGA backbone loaded with PEG. The lipophilic pyrene moiety was then replaced by the biocompatible phospholipid 1,2-distearoyl-*sn*-glycero-3-phosphoethanolamine (DSPE) by first PEGylating γPGA and then

grafting the lipophilic phospholipid moiety in the final step (see Supporting Information for methods) to afford the compound **3**. The average numbers of DSPE and PEG moieties grafted to γPGA chains were determined by ^{1}H NMR to be ~10 and ~60%, respectively.

We also synthesized a PEGylated amphiphilic polymer based on a poly(maleic anhydride-*alt*-1-octadecene) ($PMHC_{18}$) backbone. In this case, the copolymer itself contains an alternating hydrophobic unit, the C_{18} chain. Specifically, in the first synthetic step (see Supporting Information for methods), maleic anhydride groups were reacted with primary amine-terminated poly(ethylene glycol) methyl ethers (mPEG-NH_2). The remaining carboxylic acids of $PMHC_{18}$ were coupled to additional mPEG-NH_2 via EDC amidation to obtain a fully PEGylated, highly water soluble amphiphile polymer (**1**). The average number of PEG moieties grafted to $PMHC_{18}$ chains was determined by ^{1}H NMR to be ~ 200% (two molecules of mPEG per unit of $PMHC_{18}$).

All three polymers are completely soluble in both chloroform and in aqueous media. Thus, in aqueous conditions, hydrophobicity-driven self-assembly would be expected. In particular, the aqueous polymers are able to form micelles. We measured the CMC (critical micelle concentration) for each polymer (see Supporting Information Figure S1). Surface tension measurement yielded CMCs of 0.2 mg/mL for **1**, 0.3 mg/mL for **2**, and 0.4 mg/mL for **3**. Also, we used dynamic light scattering to measure the size distribution of the micelles self-assembled in water (see the Supporting Information Figures S2 and S3). The surfactant molecules' mean hydrated diameters were ~17, ~33, and ~56 nm for **1**, **2**, and **3**, respectively, whereas micelles of the polymers have hydrated diameters of ~132, ~232, and ~196 nm for **1**, **2**, and **3**, respectively.

Functionalization of Carbon Nanotubes by 1–3

Figure 2 (see also the Supporting Information Figures S5 and S6) illustrates that following sonication in polymer solutions we obtain excellent suspensions of SWNTs stabilized in water by polymers **1**–**3**, even after removal of excess polymer by repeated vacuum filtration (200 nm pore size). SWNT suspensions showed excellent stability, without aggregation or deviation of native UV/vis/NIR absorbance, at pH values ranging from 1 to 12, at high temperature overnight, and in 50% fetal calf serum for 48 h. AFM images (Figure 2b) show mostly dispersed SWNTs with lengths of ~200 nm. The UV–vis (Figure 2c) absorbance spectrum of SWNTs shows van Hove singluarities typical of well-dispersed SWNTs, with characteristic E_{11} and E_{22} transitions. The pyrene, the C_{18}, and DSPE moieties have a strong tendency to adsorb on SWNTs by hydrophobic interactions in aqueous media and, when applicable, by π-stacking. In this way, we obtain robustly coated SWNTs in aqueous media. Proof of the intimate interaction between pyrene and the NT sidewall was observed by quenching of pyrene fluorescence (see Supporting Information Figure S7) relative to free **2** with the same OD. Figure 2d shows the photoluminescence versus excitation (PLE) spectrum of SWNTs, the inherent NIR photoluminescent properties of SWNTs are retained when they are coated with **1**.

Functionalization of Gold Nanoparticles by 2 and 3

In addition to directly suspending NTs in the case of γPGA polymers (**2** and **3**), it is possible to exchange other nanostructures from their native capping ligand into our amphiphilic γPGA polymer. For example, very good suspensions of gold NPs in water were obtained through sonication for 10 min in the presence of excess **2** or **3** to displace citrate. Excess citrate was removed by dialysis, and the excess of surfactant was removed by repeated centrifugation. This procedure gave mostly dispersed nanoparticles, as shown by TEM (Figure 3a). As with NTs, this suspension was observed to be stable under various conditions, such as neutral to basic pH values, at 70 °C overnight, and in 50% serum, showing no significant changes in suspension dispersity or absorbance after a 48 h incubation. In contrast, thiol-mPEG (5 kDa), a strong and

covalent passivator of gold nanoparticles, showed less stability. In particular, as shown in (Figure 3b), the NPs-thiol-mPEG (5 kDa) are stable only in the presence of excess thiol-mPEG (see the Supporting Information Figure S9). Indeed if the excess of the thiol-mPEG is removed by centrifugation, the solution of NPs becomes unstable, forming aggregates. The UV/visible spectrum (Figure 3a) shows the absorbance of gold nanoparticles at 530 nm. In this case (see Supporting Information Figure S8), the intensity of pyrene adsorbance is dampened due to perturbations of gold nanoparticles, suggesting direct interaction of pyrene with the gold surface.[55] As in the case of NTs, the pyrene and DSPE moieties were adsorbed on the gold suface through hydrophobic interactions.

Functionalization of Gold Nanorods by 2

We also used our polymeric amphiphile to suspend gold nanorods. For example, very good suspensions of gold NRs in water were obtained through sonication for 15 min in presence of excess **2** to displace CTAB (hexadecyltrimethylammonium bromide). Excess CTAB was removed by dialysis, and the excess of surfactant was removed by repeated centrifugation. This procedure gave mostly dispersed nanorods, as shown by TEM and UV/vis absorbance spectroscopy (Figure 3c). Suspensions of gold nanorods with **2** were stable at neutral to basic pH values, at 70 °C overnight, and in 50% serum for 48 h. This result is important because nanorods with covalent thiol-based passivation are unstable under similar conditions. The UV/vis absorbance spectrum in (Figure 3c) shows the transverse and longitudinal adsorbance of gold nanorods suspended by **2** or by CTAB at 520 and 860 nm, respectively. While the solutions were originally normalized to the same OD, removal of excess surfactant causes significant aggregation and consequent loss of plasmon absorbance for CTAB-suspended NRs; however, NRs suspended by **2** remain stable, even in the presence of serum. Again, the intensity of pyrene absorbance is dampened (data not shown) by close proximity to the gold nanorods. The TEM picture shows the size distibution and dispersity of nanorods suspended with **2**.

Circulation Time of Carbon Nanotubes Functionalized by 1–3

Long blood circulation half-life of a drug carrier is desired to improve the bioavailability of the drug. For most nanomaterials, this has been an elusive goal. For example, after systemic administration, carbon nanotubes are gradually cleared from the circulating blood by macrophage uptake as part of the RES, which leads to accumulation in the liver and spleen. Therefore, prolonged circulation can only be achieved if rapid RES uptake is avoided. In our previous studies, we have shown that surface coating of SWNTs can delay RES uptake and thus increase blood circulation.[28,56,57]

Hypothesizing that the pronounced PEG loading on the polymer SWNTs would prolong the blood circulation, we injected these conjugates into mice. Importantly, we observed (Figure 4a) a circulation half-life of 2.4 h for SWNTs coated with **3**, a very long circulation half-life of 22.1 h for SWNTs coated with **2**, and 18.9 h for SWNTs coated with **1**, which were far longer than values reported by others, as well as our previous data obtained for DSPE-coupled linear PEG-coated SWNTs (0.33 h for DSPE-l-2kPEG, 2.4 h for DSPE-l-5kPEG, Figure 4b) or DSPE-branched PEG functionalized SWNTs (5.4 h for DSPE-br-7kPEG, Figure 4a,b).[28] While the packing density of PEG coatings immobilized on nanotubes via conventional surfactants with single anchoring points is limited by steric hindrance, the multiple lipophilic anchoring domains and multiple PEG chains of **2** and **1** allow continuous binding of the polymer onto the nanotube surface, yielding a highly dense PEG coating. Additionally, the molecular weight and functionalization density of each PEG branch was important for obtaining long circulation. Similar surfactants produced with mPEG 0.75 kDa in lieu of 5 kDa led to significantly reduced circulation times. Moreover, functionalization of the γPGA backbone with less than 50% of mPEG 5 kDa gave unsatisfactory circulation results. Thus, not only does this unique polymer coating hold promise for potential in vivo therapeutic applications, we

have also been able to discern what aspects of the polymer lead to desirable properties in our SWNT conjugates.

Conclusion

In conclusion, we report the synthesis of new versatile PEGylated branched polymers that provide stable suspensions of carbon nanotubes, gold nanoparticles, and gold nanorods. We used poly-γ-glutamic acid (γPGA) functionalized with either pyrene moieties or phospholipids to provide robust polymer–particle interactions and PEG, enhancing aqueous solubility and biocompatibility. We also used PEGylated poly(maleic anhydride-*alt*-1-octadecene) ($PMHC_{18}$) to provide very stable suspensions of carbon nanotubes. We showed that the SWNTs, Au NPs, and Au NRs functionalized by these polymers show excellent stability in aqueous solutions, at different pH values, and elevated temperatures, as well as in serum. Moreover, the polymer-coated SWNTs exhibit unprecedentedly long blood circulation (half-life 22.1 h for **2** and 18.9 h for **1**) upon intravenous injection into mice, far exceeding the previous record for circulation half-life of 5.4 h. All these characteristics make these very powerful materials for in vivo applications, including drug delivery or imaging.

References

1. Sinha N, Yeow JTW. IEEE Trans Nanobiosci 2005;4(2):180–195.
2. Han G, Ghosh P, Rotello VM. Nanomedicine 2007;2(1):113–123. [PubMed: 17716197]
3. Kogan MJ, Olmedo I, Hosta L, Guerrero AR, Cruz LJ, Albericio F. Nanomedicine 2007;2(3):287–306. [PubMed: 17716175]
4. Kam NWS, O'Connell M, Wisdom JA, Dai HJ. Proc Natl Acad Sci USA 2005;102(33):11600–11605. [PubMed: 16087878]
5. Kam NWS, Liu ZA, Dai HJ. Angew Chem, Int Ed 2006;45(4):577–581.
6. Williams KA, Veenhuizen PTM, de la Torre BG, Eritja R, Dekker C. Nature 2002;420(6917):761–761. [PubMed: 12490938]
7. Thaxton CS, Georganopoulou DG, Mirkin CA. Clin Chim Acta 2006;363(1–2):120–126. [PubMed: 16214124]
8. Maubach G, Csaki A, Born D, Fritzsche W. Nanotechnology 2003;14(5):546–550.
9. Kryachko ES, Remacle F. Nano Lett 2005;5(4):735–739. [PubMed: 15826118]
10. Nath N, Chilkoti A. J Fluoresc 2004;14(4):377–389. [PubMed: 15617380]
11. Nam JM, Thaxton CS, Mirkin CA. Science 2003;301(5641):1884–1886. [PubMed: 14512622]
12. Chen Z, Tabakman SM, Goodwin AP, Kattah MG, Daranciang D, Wang X, Zhang G, Li X, Liu Z, Utz PJ, Jiang K, Fan S, Dai H. Nat Biotechnol 2008;26(11):1285–1292. [PubMed: 18953353]
13. Liu Z, Cai WB, He LN, Nakayama N, Chen K, Sun XM, Chen XY, Dai HJ. Nat Nanotechnol 2007;2(1):47–52. [PubMed: 18654207]
14. Adams ML, Lavasanifar A, Kwon GS. J Pharm Sci 2003;92(7):1343–1355. [PubMed: 12820139]
15. Yang ST, Fernando KAS, Liu JH, Wang J, Sun HF, Liu YF, Chen M, Huang YP, Wang X, Wang HF, Sun YP. Small 2008;4(7):940–944. [PubMed: 18574799]
16. Xiaoming Sun ZL, Welsher K, Robinson JT, Goodwin A, Zaric S, Dai AH. Nano Res 2008;1:203–212.
17. Lin Wang WZ. Nano Res 2008;1:99–115.
18. Welsher K, Liu Z, Daranciang D, Dai H. Nano Lett 2008;8(2):586–590. [PubMed: 18197719]
19. O'Connell MJ, Bachilo SM, Huffman CB, Moore VC, Strano MS, Haroz EH, Rialon KL, Boul PJ, Noon WH, Kittrell C, Ma JP, Hauge RH, Weisman RB, Smalley RE. Science 2002;297(5581):593–596. [PubMed: 12142535]
20. Richard C, Balavoine F, Schultz P, Ebbesen TW, Mioskowski C. Science 2003;300(5620):775–778. [PubMed: 12730595]

21. Numata M, Asai M, Kaneko K, Bae AH, Hasegawa T, Sakurai K, Shinkai S. J Am Chem Soc 2005;127 (16):5875–5884. [PubMed: 15839686]
22. Dieckmann GR, Dalton AB, Johnson PA, Razal J, Chen J, Giordano GM, Munoz E, Musselman IH, Baughman RH, Draper RK. J Am Chem Soc 2003;125(7):1770–1777. [PubMed: 12580602]
23. Karajanagi SS, Yang HC, Asuri P, Sellitto E, Dordick JS, Kane RS. Langmuir 2006;22(4):1392–1395. [PubMed: 16460050]
24. Zheng M, Jagota A, Semke ED, Diner BA, Mclean RS, Lustig SR, Richardson RE, Tassi NG. Nat Mater 2003;2(5):338–342. [PubMed: 12692536]
25. Zheng M, Jagota A, Strano MS, Santos AP, Barone P, Chou SG, Diner BA, Dresselhaus MS, McLean RS, Onoa GB, Samsonidze GG, Semke ED, Usrey M, Walls DJ. Science 2003;302(5650):1545–1548. [PubMed: 14645843]
26. Sinani VA, Gheith MK, Yaroslavov AA, Rakhnyanskaya AA, Sun K, Mamedov AA, Wicksted JP, Kotov NA. J Am Chem Soc 2005;127(10):3463–3472. [PubMed: 15755166]
27. Chatterjee T, Yurekli K, Hadjiev VG, Krishnamoorti R. Adv Funct Mater 2005;15(11):1832–1838.
28. Liu Z, Davis C, Cai WB, He L, Chen XY, Dai HJ. Proc Natl Acad Sci USA 2008;105(5):1410–1415. [PubMed: 18230737]
29. Cheng Y, Samia AC, Meyers JD, Panagopoulos I, Fei BW, Burda C. J Am Chem Soc 2008;130(32): 10643–10647. [PubMed: 18642918]
30. Huff TB, Hansen MN, Zhao Y, Cheng JX, Wei A. Langmuir 2007;23(4):1596–1599. [PubMed: 17279633]
31. Oyelere AK, Chen PC, Huang XH, El-Sayed IH, El-Sayed MA. Bioconjugate Chem 2007;18(5): 1490–1497.
32. Sonnichsen C, Reinhard BM, Liphardt J, Alivisatos AP. Nat Biotechnol 2005;23(6):741–745. [PubMed: 15908940]
33. Cognet L, Tardin C, Boyer D, Choquet D, Tamarat P, Lounis B. Proc Natl Acad Sci USA 2003;100 (20):11350–11355. [PubMed: 13679586]
34. Schultz S, Smith DR, Mock JJ, Schultz DA. Proc Natl Acad Sci USA 2000;97(3):996–1001. [PubMed: 10655473]
35. Tong L, Zhao Y, Huff TB, Hansen MN, Wei A, Cheng JX. Adv Mater 2007;19(20):3136–3141. [PubMed: 19020672]
36. Paciotti GF, Myer L, Weinreich D, Goia D, Pavel N, McLaughlin RE, Tamarkin L. Drug Delivery 2004;11(3):169–183. [PubMed: 15204636]
37. Gao MY, Kirstein S, Mohwald H, Rogach AL, Kornowski A, Eychmuller A, Weller H. J Phys Chem B 1998;102(43):8360–8363.
38. Chan WCW, Nie SM. Science 1998;281(5385):2016–2018. [PubMed: 9748158]
39. Pinaud F, King D, Moore HP, Weiss S. J Am Chem Soc 2004;126(19):6115–6123. [PubMed: 15137777]
40. Kanaras AG, Kamounah FS, Schaumburg K, Kiely CJ, Brust M. Chem Commun 2002;(20):2294–2295.
41. Jiang W, Mardyani S, Fischer H, Chan WCW. Chem Mater 2006;18(4):872–878.
42. Dubertret B, Skourides P, Norris DJ, Noireaux V, Brivanlou AH, Libchaber A. Science 2002;298 (5599):1759–1762. [PubMed: 12459582]
43. Fan HY, Leve EW, Scullin C, Gabaldon J, Tallant D, Bunge S, Boyle T, Wilson MC, Brinker CJ. Nano Lett 2005;5(4):645–648. [PubMed: 15826102]
44. Mulder WJM, Koole R, Brandwijk RJ, Storm G, Chin PTK, Strijkers GJ, Donega CD, Nicolay K, Griffioen AW. Nano Lett 2006;6(1):1–6. [PubMed: 16402777]
45. LizMarzan LM, Giersig M, Mulvaney P. Chem Commun 1996;(6):731–732.
46. Bruchez M, Moronne M, Gin P, Weiss S, Alivisatos AP. Science 1998;281(5385):2013–2016. [PubMed: 9748157]
47. Gerion D, Pinaud F, Williams SC, Parak WJ, Zanchet D, Weiss S, Alivisatos AP. J Phys Chem B 2001;105(37):8861–8871.
48. Selvan ST, Tan TT, Ying JY. Adv Mater 2005;17(13):1620–1625.

49. Zhelev Z, Ohba H, Bakalova R. J Am Chem Soc 2006;128(19):6324–6325. [PubMed: 16683790]
50. Sohn BH, Choi JM, Yoo SI, Yun SH, Zin WC, Jung JC, Kanehara M, Hirata T, Teranishi T. J Am Chem Soc 2003;125(21):6368–6369. [PubMed: 12785767]
51. Porta F, Prati L, Rossi M, Scari G. Colloids Surf A 2002;211(1):43–48.
52. Markowitz MA, Dunn DN, Chow GM, Zhang J. J Colloid Interface Sci 1999;210(1):73–85. [PubMed: 9924109]
53. Chen RJ, Zhang YG, Wang DW, Dai HJ. J Am Chem Soc 2001;123(16):3838–3839. [PubMed: 11457124]
54. Liu WH, Choi HS, Zimmer JP, Tanaka E, Frangioni JV, Bawendi M. J Am Chem Soc 2007;129(47): 14530–14531. [PubMed: 17983223]
55. Ipe BI, Thomas KG. J Phys Chem B 2004;108(35):13265–13272.
56. Wang D, Ji WX, Li ZC, Chen LW. J Am Chem Soc 2006;128(20):6556–6557. [PubMed: 16704245]
57. Nakayama-Ratchford N, Bangsaruntip S, Sun XM, Welsher K, Dai HJ. J Am Chem Soc 2007;129 (9):2448–2449. [PubMed: 17284037]
58. Ashiuchi M, Nawa C, Kamei T, Song JS, Hong SP, Sung MH, Soda K, Yagi T, Misono H. Eur J Biochem 2001;268(22):6003–6003.
59. Parveen S, Sahoo SK. Clin Pharmacokinet 2006;45(10):965–988. [PubMed: 16984211]

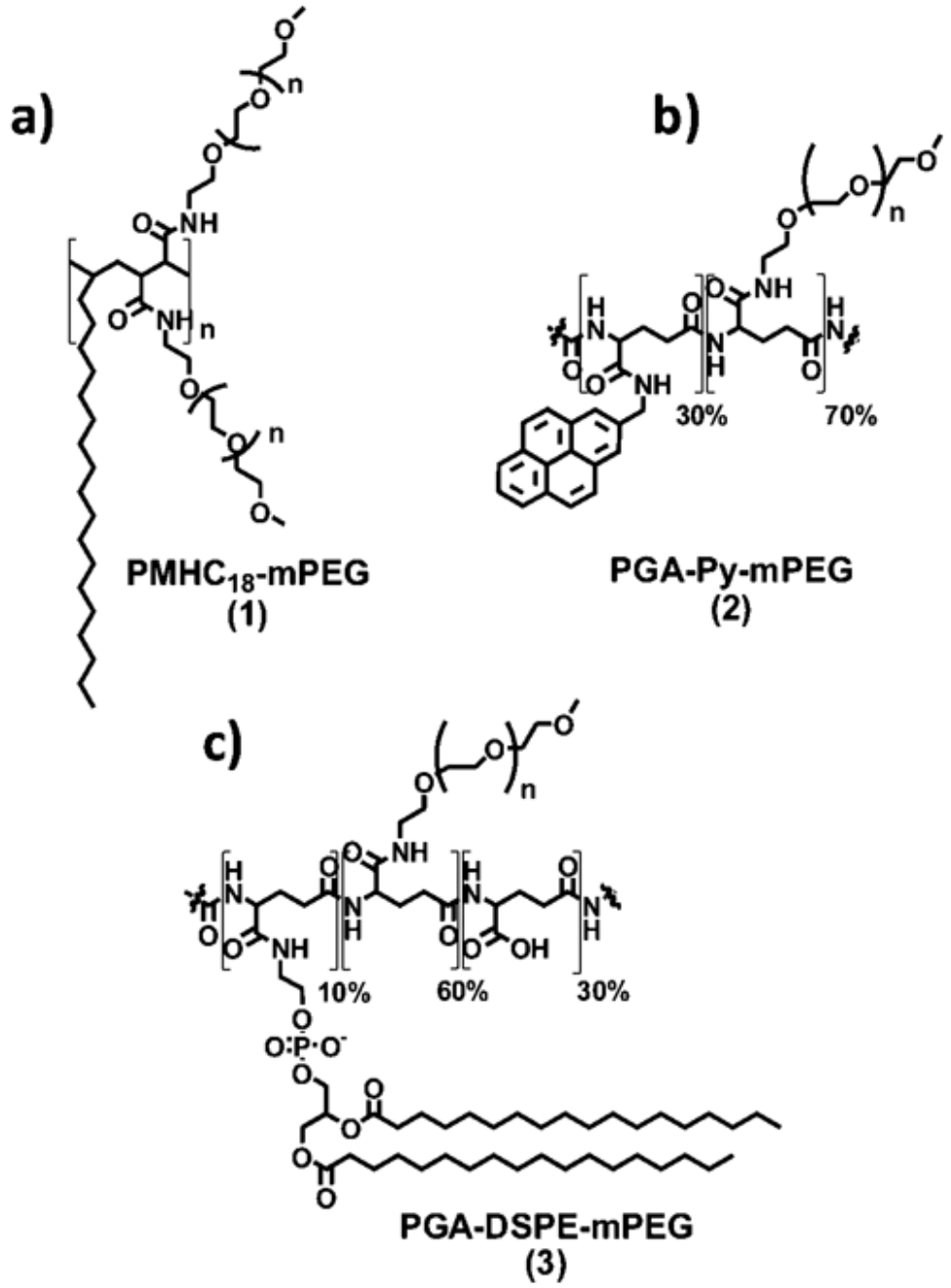

Figure 1.

(a) $PMHC_{18}$-mPEG (**1**): poly(maleic anhydride-*alt*-1-octadecene)-poly(ethylene glycol) methyl ethers). (b) γPGA-Py-mPEG (**2**): poly-(γglutamic acid)-pyrine(30%)-poly(ethylene glycol) methyl ethers) (70%). (c) γPGA-DSPE-mPEG (**3**): poly-(γ-glutamic acid)-phospholipid 1,2-distearoyl-*sn*-glycero-3-phosphoethanolamine (10%)-poly(ethylene glycol) methyl ethers) (60%).

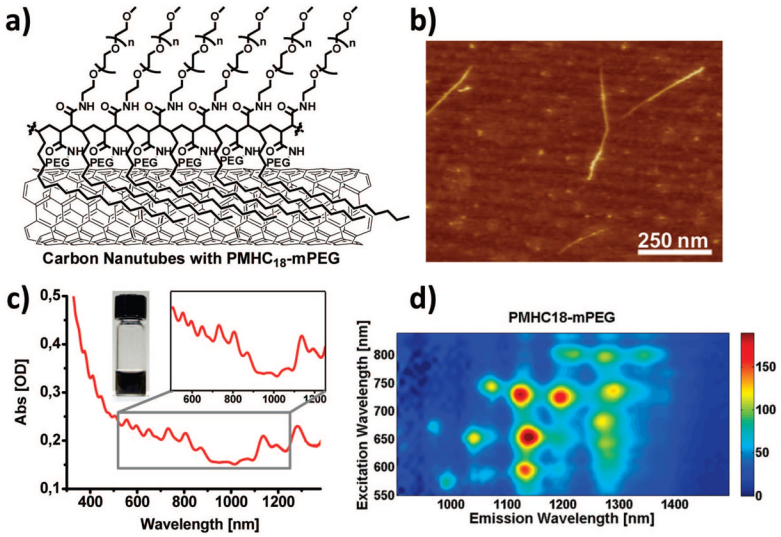

Figure 2.

(a) Single-walled carbon nanotubes (SWNTs) coated with **1**. (b) AFM image of SWNTs with **1** coating. Non-uniform height along the nanotube is attributed to the presence of the polymer coating. (c) UV–vis–NIR absorption spectrum of SWNTs with **1** coating following excess polymer removal. Inset: Digital photograph of a SWNT suspension. (d) Photoluminescence versus excitation (PLE) spectrum of SWNTs with **1** coating. Horizontal axis shows photoluminescence spectrum at different excitations along the vertical axis. Bright spots correspond to semiconducting SWNTs of different chiralities, demonstrating that the inherent NIR photoluminescent properties are retained with **1** coating.

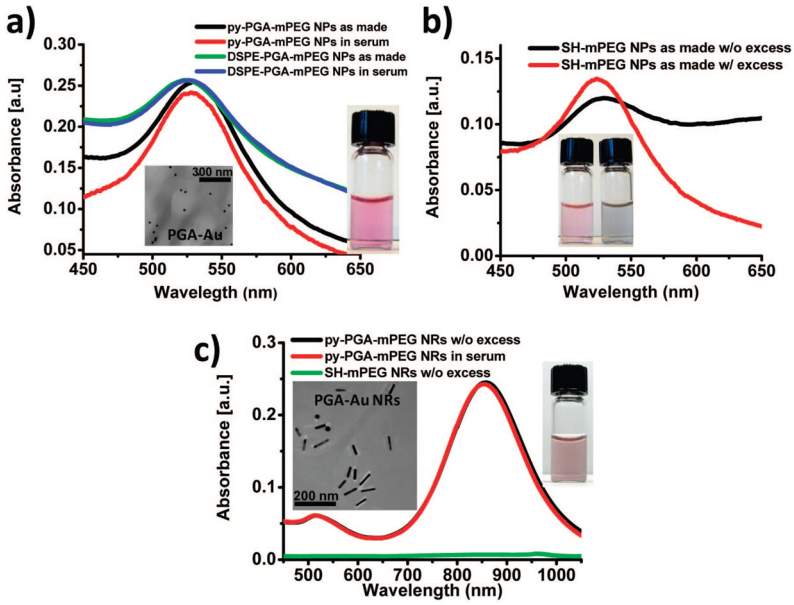

Figure 3.

(a) UV–vis absorption data of 20 nm gold nanoparticles with **2** (inset: solution photo) or **3** coating in 50% fetal calf serum and as made (in water). Inset: TEM image of 20 nm Au NPs stabilized by **2**. The UV–vis spectra show the plasmon peak of gold nanoparticles at 530 nm in various coatings and media. (b) The 20 nm gold nanoparticles with to SH-mPEG (5 kDa) coating with (left) and without (right) excess of SH-mPEG, showing aggregation following excess removal. (c) Gold nanorods with **2** coating as made (in water, without excess of surfactant, solution photo) and in 50% fetal calf serum; gold nanorods with SH-mPEG (5 kDa) coating (in water, without excess of surfactant). All Au NR suspensions were normalized in OD to the plasmon peak at 860 nm before removal of excess surfactant. Inset: TEM images of Au NRs stabilized by **2**. The UV–vis–NIR spectrum shows the transverse and longitudinal plasmon peaks of gold nanorods at 520 and 860 nm, respectively.

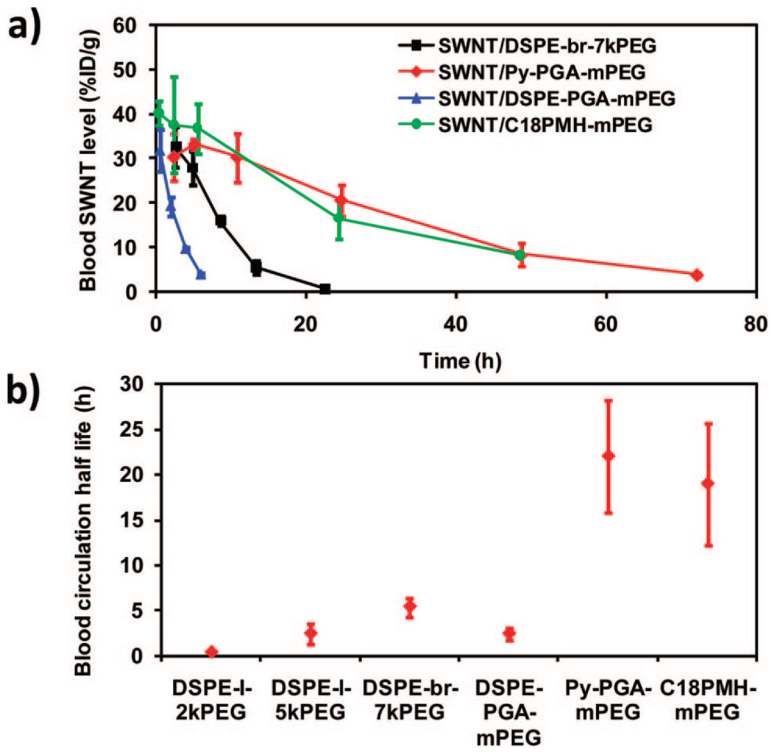

Figure 4.

Blood circulation data of SWNTs with different functionalizations in balb/c mice. (a) Blood circulation curves of **1**–**3** coated nanotubes compared with DSPE-branched-7kPEG coated nanotubes. The latter one was previously reported by our group.[28] Error bars were based on three mice per group at each time point (0.5, 2, 5, 10, 24, 48, 72 h). (b) Blood circulation half-lives of different SWNTs obtained by first-order decay fitting of all data points. SWNTs with **1** and **2** coating exhibited drastically prolonged circulation half-life compared with previous DSPE-PEG functionalized nanotubes.